Hindawi
International Journal of Photoenergy
Volume 2019, Article ID 5986874, 12 pages
https://doi.org/10.1155/2019/5986874

Research Article

Investigation of Daytime Peak Loads to Improve the Power Generation Costs of Solar-Integrated Power Systems

Stephen Afonaa-Mensah[1,2] **Qian Wang**[1] **and Benjamin B. Uzoejinwa**[1,3]

[1]*School of Energy and Power Engineering, Jiangsu University, Zhenjiang 212013, China*
[2]*Department of Electrical/Electronic Engineering, Takoradi Technical University, P.O. Box 256, Takoradi, Ghana*
[3]*Department of Agricultural and Bioresources Engineering, University of Nigeria, Nsukka, 41001 Enugu State, Nigeria*

Correspondence should be addressed to Qian Wang; qwang@ujs.edu.cn

Received 20 March 2019; Revised 10 July 2019; Accepted 3 October 2019; Published 11 November 2019

Academic Editor: Pierluigi Guerriero

Improving daytime loads can mitigate some of the challenges posed by solar variations in solar-integrated power systems. Thus, this simulation study investigated the different levels of daytime peak loads under varying solar penetration conditions in solar-integrated power systems to improve power generation cost performance based on different load profiles and to mitigate the challenges encountered due to solar variation. The daytime peak loads during solar photovoltaic generation hours were determined by measuring the solar load correlation coefficients between each load profile and the solar irradiation, and the generation costs were determined using a dynamic economic dispatch method with particle swarm optimization in a MATLAB environment. The results revealed that the lowest generation costs were generally associated with load profiles that had low solar load correlation coefficients. Conversely, the load profile with the highest positive solar load correlation coefficient exhibited the highest generation costs, which were mainly associated with violations of the supply-demand balance requirement. However, this profile also exhibited the lowest generation costs at high levels of solar penetration. This result indicates that improving daytime load management could improve generation costs under high solar penetration conditions. However, if the generation system lacks sufficient ramping capability, this technique could pose operational challenges that adversely impact power generation costs.

1. Introduction

Recent reforms in the power sector have contributed to the dramatic rise in the deployment of solar photovoltaics (PV) to meet human energy needs. As a renewable energy (RE) source, solar PV has played a significant role in finding solutions to the global challenge of providing a sustainable energy supply to meet rising energy demands [1, 2].

However, the penetration of solar PV into power systems is not without challenges. A typical problem encountered in the utilization of solar PV is that it is a variable RE source; this characteristic can adversely affect the performance of the power systems into which they are integrated [3]. The adverse effects of solar PV variation on power systems include frequency deviation, voltage fluctuations, and blackouts [4, 5].

Mitigating the challenges posed by the variable nature of solar PV requires the combined efforts of both the supply and demand sides of the power system. The solar variation mitigation techniques that have been explored include generation reserves, storage facilities, interconnected grids, and demand response programmes [6].

Among the solar variation mitigation techniques on the demand side, several studies have shown that increasing the daytime loads in solar-integrated power systems can alleviate some of the challenges associated with solar variation. For instance, Stodola and Modi [7] demonstrated that investments in storage facilities can be reduced by increasing the daytime loads in solar PV-integrated systems and replacing one quarter of the power supplied from dispatchable generators with solar PV without using storage systems. Similarly, Hasan and Chowdhury [8]

reported that improving the daytime loads of solar-integrated systems can lessen the requirements for storage facilities and subsequently decrease power generation costs. Another study [9] showed that shifting the loads to solar power production hours improved the efficiency of storage facilities and the utilization of the solar power generated. In [10], it was reported that improving the daytime loads economically favoured solar-integrated systems. Moreover, Bilal et al. [11] demonstrated that load profiles with high daytime loads resulted in a lower levelized cost of energy (LCOE) than other load profiles. Other studies focusing on the impact of improving daytime loads on generator performance reported that this technique reduced ramping in dispatchable generation units [12]. Similarly, to address the "duck curve" phenomenon, Bayram et al. [13] demonstrated that, at high solar penetration levels, less ramping was required in dispatchable generators in load profiles with peak loads coinciding with solar PV generation than in those in other load profiles. Other studies have reported that the performance of variable RE sources such as solar PV is significantly affected by the proportion of the load demand during RE generation periods [2, 14].

Several studies have shown that the penetration of variable RE sources such as solar PV into power systems significantly alters the original load characteristics [15–18]. In this regard, Asare-Bediako et al. [17] showed that the high penetration of solar PV contributed to the deviation of load profiles from classical patterns. Johnson et al. [15] revealed that the high penetration of solar PV altered the initial load peak hours and, consequently, the distribution of power cost among various classes of electricity consumers. Additionally, the study in Ref. [16] demonstrated that the changes in the characteristics of load profiles as PV penetration increased affected the ramping requirements in the power generation units. According to Helman [2], the resulting impact of solar PV on the load profile is the key in the operational evaluation and capacity valuation of solar-integrated power systems. Moreover, another study [18] demonstrated that the changes in load characteristics caused by the variable RE sources affect the operational costs of power systems. Thus, with the increasing penetration of solar PV into power systems and the consequential impact on load characteristics, information regarding the generation cost performance of daytime load solar variation mitigation techniques is vital for the power industry.

However, to the best of our knowledge, existing works on using daytime loads as solar variation mitigation techniques to improve the performance of solar-integrated power systems have not clearly provided this key information. Thus, the main contribution of this study is to improve the generation costs of solar-integrated power systems by investigating the generation cost performance of load profiles at various levels of daytime peak loads under varying solar penetration conditions to mitigate the challenges related to solar variation. Thus, in this study, the daytime peak loads during solar PV generation hours were determined by measuring the solar load correlation coefficients between the load profile and the solar irradiation, and the dynamic economic dispatch (DED) method with particle swarm optimization (PSO) was used to model the generation costs of the solar-integrated power systems.

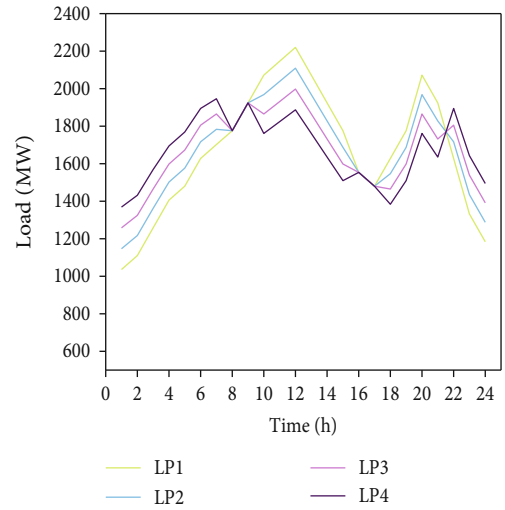

Figure 1: Twenty-four-hour load profiles (LPs).

2. Materials and Methods

This simulation study was conducted in a test system with ten thermal generation units in a MATLAB environment (MATLAB r2016a, MathWorks®, Natick, MA, USA). The initial load profile (LP1), which had a considerably high daytime load, was obtained from [19] (Figure 1). However, to vary the level of daytime load, 5% of the peak load of the initial load profile was continuously shifted from the peak period to the valley period to obtain the other load profiles (i.e., LP2-LP4). In this study, the peak periods were assumed to be within the hours from 10 h to 15 h and from 18 h to 21 h and that the valley periods were from 1 h to 7 h and from 22 h to 24 h. Additionally, during the load-shifting process, it was ensured that the net sums of the loads of all load profiles were equal.

Additionally, the costs of the load-shifting process were assumed to be negligible. This assumption facilitates the exploration of the main objective of this study, which is to evaluate the impacts of the various load profiles themselves on the power generation costs. This assumption allows these effects to be clearly observed without other cost components, such as the cost of load shifting, influencing the results. Nonetheless, this assumption could be a limitation of the study because load shifting can require considerable costs in power system operation.

3. Problem Formulation

In this study, the generation cost of a solar-integrated power system was formulated as a single-objective 24 h DED optimization task. Thus, the objective of the DED employed in this study was to minimize the generation cost of the online generation units for the given load demands while

considering the operational constraints over the dispatch period. The DED was modelled as follows [20–22].

3.1. Objective Function. The objective function was formulated as [20]

$$\min \text{FC} + \text{SC} + \text{LC}, \tag{1}$$

where

$$\text{FC} = \sum_{t=1}^{T}\sum_{i=1}^{N} F_{i,t}(P_{i,t}), \tag{2}$$

where FC is the power generation cost of all the thermal generation units over the dispatch period, T is the total number of dispatch time intervals, N is the total number of thermal generation units, and $F_{i,t}(P_{i,t})$ is the fuel cost function of the i^{th} thermal generation unit with real power output $P_{i,t}$ during time interval t.

The fuel cost function, which considers the valve-point loading effect, was formulated as shown in

$$F_{i,t}(P_{i,t}) = a_i(P_{i,t})^2 + b_iP_{i,t} + c_i + \left|e_i \sin\left(f_i(P_{i\,\min} - P_{i,t})\right)\right|, \tag{3}$$

where a_i, b_i, and c_i are the fuel cost coefficients of the i^{th} thermal generation unit and e_i and f_i are constants of the valve-point loading effect.

Moreover, the cost of solar power SC, was estimated as [21]

$$\text{SC} = \sum_{t=1}^{T}\sum_{m=1}^{M} S_{m,t}(P_{m,t}), \tag{4}$$

where M is the total number of solar power generation units and $S_{m,t}(P_{m,t})$ is the solar power cost function of the m^{th} solar power generation unit with power output $P_{m,t}$ during the t^{th} time interval.

$$\begin{aligned} S_{m,t}(P_{m,t}) &= aI^PP_{m,t} + G^EP_{m,t}, \\ a &= \frac{r}{\left(1-(1+r)^{-N}\right)}. \end{aligned} \tag{5}$$

Here, I^P and G^E are the investment cost and the operation and maintenance cost, respectively, per unit of installed power ($/MW) of the m^{th} solar power generation unit. Additionally, a, r, and N are the annuitization coefficient, interest rate, and investment lifetime of the solar power generation units, respectively.

Equation (6) expresses the cost of the load-shifting process, LC:

$$\text{LC} = \sum_{t=1}^{T}\sum_{k=1}^{K} u_{k,t}L_{k,t}, \tag{6}$$

where K is the total number of regulated loads in the load-shifting process, $L_{k,t}$ is the shifted load in the k^{th}-regulated load within time interval t, and $u_{k,t}$ is the cost coefficient of load shifting in the k^{th}-regulated load within the t^{th} time interval.

3.2. Constraints. The DED was subject to the following equality and inequality constraints.

(i) Power supply-demand balance constraints

$$\sum_{i=1}^{N} P_{i,t} + \sum_{m=1}^{M} S_{m,t} + \sum_{k=1}^{K} L_{k,t} = P_{D,t} + P_{L,t}, \tag{7}$$

where $P_{D,t}$ is the load demand during the t^{th} time interval and $P_{L,t}$ represents the transmission losses during the t^{th} time interval. The transmission losses were determined using the B-loss coefficient method shown in

$$P_{L,t} = \sum_{i=1}^{N}\sum_{j=1}^{N} P_{i,t}B(i,j)P_{j,t}, \tag{8}$$

where $P_{i,t}$ and $P_{j,t}$ are the real power outputs of the i^{th} and j^{th} generation units in time interval t, respectively, and $B(i,j)$ is the transmission loss coefficient

(ii) Generator power limits

The minimum $(P_{i\,\min})$ and maximum $(P_{i\,\max})$ real power outputs of the i^{th} generation unit were constrained as follows:

$$P_{i\,\min} \le P_{i,t} \le P_{i\,\max} \tag{9}$$

(iii) Ramping limits

The ramping limits of the generation units were considered based on the following formula:

$$\max\left(P_{i\,\min}, P_{i,t-1} - DR_i\right) \le P_{i,t} \le \min\left(P_{i\,\max}, P_{i,t-1} + UR_i\right), \tag{10}$$

where UR_i and DR_i are the ramp-up and ramp-down limits of the i^{th} thermal generation unit, respectively

3.3. Load-Shifting Formulation and Constraints. The load demand during the load-shifting process was formulated as shown in equations (11) and (12) [23]:

$$P_{DRt} = P_{Dt} + l_t, \tag{11}$$

$$l_t = P_{Dt} \times DR_t, \tag{12}$$

where P_{DRt} is the load demand during the load-shifting process in time interval t, P_{Dt} is the initial load demand at time t, l_t is the load demand that can be shifted during time interval t, and DR_t is the participation factor of the

load demand in the load-shifting process during the t^{th} time interval.

Equation (13) ensures that the total load shifted during the entire dispatch period is zero.

$$\sum_{t=1}^{T} l_t = 0. \tag{13}$$

Additionally, the participation factor of the load demand was subject to the following inequality constraint:

$$DR_{t\ \min} \le DR_t \le DR_{t\ \max}, \tag{14}$$

where $DR_{t\ \min}$ and $DR_{t\ \max}$ represent the minimum and maximum participation factors in the load-shifting process, respectively.

3.4. Solar PV System. The output energy E_o of the solar PV system was estimated as follows:

$$\begin{aligned} E_o &= E_h \times \eta_{\text{sub}} \times \eta_{\text{inv}}, \\ E_h &= P_{\text{array}} \times H_i, \\ P_{\text{array}} &= P_{\text{stc}} \times f_{\text{temp}} \times f_{\text{dirt}} \times f_{\text{man}}, \end{aligned} \tag{15}$$

where E_h is the hourly output energy of the solar PV system, η_{sub} and η_{inv} are the subsystem and inverter efficiencies, respectively, H_i is the hourly solar irradiation, P_{array} and P_{stc} are the derated and rated output powers of the solar PV system, respectively, and f_{temp}, f_{dirt}, and f_{man} represent losses due to the temperature of the solar PV system, dirt, and manufacturer tolerances, respectively [24]. It is worth noting that E_o also represents the average output power of the solar PV system within the dispatch period considered in this study.

3.5. Particle Swarm Optimization. PSO is a metaheuristic algorithm that operates with swarm particles. Each particle in the swarm is characterized by a randomly assigned position and velocity in the solution search space. At every iteration, the velocity and position of the particles are evaluated by an objective function. Subsequently, each particle uses its own previous best position (pbest_i) and that of the swarm (gbest) to continuously update its velocity and position until a given criterion is met. The particle velocity and position are updated by equations (16) and (17), respectively [25]:

$$\begin{aligned} v_i(k+1) = w \times v_i(k) &+ c_1.r_1().(\text{pbest}_i - x_i(k)) \\ &+ c_2.r_2().(\text{gbest} - x_i(k)), \end{aligned} \tag{16}$$

$$x_i(k+1) = x_i(k) + v_i(k+1), \tag{17}$$

where i is the particle index, k is the iteration number, $v_i(k)$ and $x_i(k)$ are the velocity and position of the i^{th} particle at iteration k, respectively, w is an inertia weight, c_1 and c_2 are cognitive and social parameters, respectively, and r_1 and r_1 are uniform random numbers in the range [0, 1]. This study also considered $w = 1$ and $c_1 = c_2 = 2$ [25]. Moreover, the iteration number and population size of the swarm were considered to be 200 and 100, respectively. The PSO was used as the optimizer to minimize the power generation cost. Thus, the PSO was used to compute the optimal generation costs of the 24 h DED task of the solar-integrated power system for the various load profiles.

3.6. Test Systems. A test system with ten thermal generation units adopted from [19] was considered in this simulation study. The characteristics of the ten thermal generation units are presented in Table 1. Likewise, the transmission loss coefficient, B_{ij}, adopted from [26], is shown in equation (18).

$$B_{ij} = \begin{vmatrix} 0.49 & 0.14 & 0.15 & 0.15 & 0.16 & 0.17 & 0.17 & 0.18 & 0.19 & 0.20 \\ 0.14 & 0.45 & 0.16 & 0.16 & 0.17 & 0.15 & 0.15 & 0.16 & 0.18 & 0.18 \\ 0.15 & 0.16 & 0.39 & 0.10 & 0.12 & 0.12 & 0.14 & 0.14 & 0.16 & 0.16 \\ 0.15 & 0.16 & 0.10 & 0.40 & 0.14 & 0.10 & 0.11 & 0.12 & 0.14 & 0.15 \\ 0.16 & 0.17 & 0.12 & 0.14 & 0.35 & 0.11 & 0.13 & 0.13 & 0.15 & 0.16 \\ 0.17 & 0.15 & 0.12 & 0.10 & 0.11 & 0.36 & 0.12 & 0.12 & 0.14 & 0.15 \\ 0.17 & 0.15 & 0.14 & 0.11 & 0.13 & 0.12 & 0.38 & 0.16 & 0.16 & 0.18 \\ 0.18 & 0.16 & 0.14 & 0.12 & 0.13 & 0.12 & 0.16 & 0.40 & 0.15 & 0.16 \\ 0.19 & 0.18 & 0.16 & 0.14 & 0.15 & 0.14 & 0.16 & 0.15 & 0.42 & 0.16 \\ 0.20 & 0.18 & 0.16 & 0.15 & 0.16 & 0.15 & 0.18 & 0.16 & 0.19 & 0.44 \end{vmatrix} \times 0.001/\text{MW}. \tag{18}$$

Table 1: Characteristics of the ten thermal generation units [19].

Unit	Power limits		Fuel cost coefficients					Ramp rate limits	
	$P_{i\ \min}$(MW)	$P_{i\ \max}$(MW)	a_i	b_i	c_i	e_i	f_i	UR (MW/h)	DR (MW/h)
1	150	470	0.00043	21.6	958.2	450	0.041	80	80
2	135	460	0.00063	21.05	1313.6	600	0.036	80	80
3	73	340	0.00039	20.81	604.97	320	0.028	80	80
4	60	300	0.0007	23.9	471.6	260	0.052	50	50
5	73	243	0.00079	21.62	480.29	280	0.063	50	50
6	57	160	0.00056	17.87	601.75	310	0.048	50	50
7	20	130	0.00211	16.51	502.7	300	0.086	30	30
8	47	120	0.0048	23.23	639.4	340	0.082	30	30
9	20	80	0.10908	19.58	455.6	270	0.098	30	30
10	55	55	0.00951	22.54	692.4	380	0.094	30	30

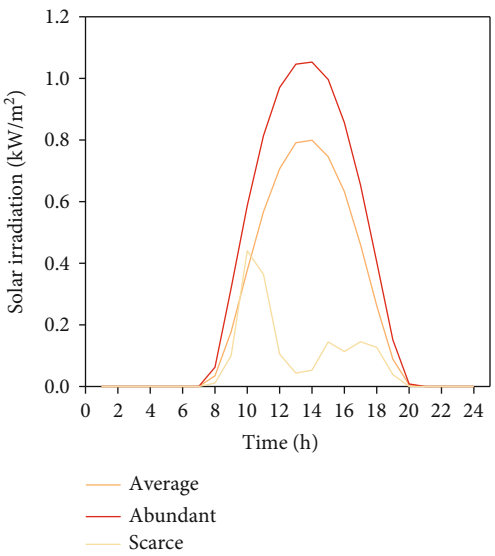

Figure 2: Twenty-four-hour solar irradiation in Wa, Ghana (location: 10°1′N and 2°5′W; source: Wa-Polytechnic weather station, Ghana).

Table 2: Solar PV system sizing considerations and parameters.

Solar panel	CS6X-300P
Shading loss	5%
Voltage drop	3%
Dirt loss	8%
Temperature loss	16.8%
Inverter efficiency	96%
Manufacturer's tolerances	3%
Maximum design temperature	39°C

Table 3: Solar power cost data [21].

Quantity	Value
Interest rate (base case)	0.09
Investment lifetime	20 years
Investment cost/unit installed	$5000/kW
Operation and maintenance cost	1.6 cents/kW

3.7. Solar Data and PV System Considerations. The solar resources in Wa, Ghana, were considered for this study. Thus, Figure 2 shows the twenty-four-hour solar irradiation in Wa, Ghana, for the average, abundant, and scarce solar resource conditions. The total solar resource is based on two years of ground-measured data. In this study, solar penetration levels from 0% to 30% in increments of 10% were considered. The solar penetration levels were estimated as percentages of the peak load demand of the initial load profile (i.e., LP1). The solar PV system sizing considerations and parameters and cost data adopted from [21] are reported in Tables 2 and 3, respectively.

3.8. Solar Load Correlation Coefficients and P Values of Load Profiles. In this study, the daytime loads within the solar PV generation hours were determined based on the solar load correlation coefficients between the various load profiles and solar irradiation under average, abundant, and scarce solar resource conditions. Thus, Table 4 shows the results of the solar load correlation coefficients and P values of the various load profiles obtained via statistical analyses of the average, abundant, and scarce solar resource conditions. The results of the 2-tailed statistical tests showed that the correlation coefficients of the load profiles, LP1 and LP2, were significant ($P = 0.05$ and 0.01) under all solar resource conditions; however, the correlation coefficients of LP3 and LP4 were not significant ($P = 0.05$ and 0.01) under all solar resource conditions.

3.9. Validation Test. A test system with six thermal generation units was used to validate the effectiveness of the power generation cost optimization algorithm. The characteristics of the six thermal generation units, the 24 h load profile, and the transmission loss coefficient adopted from [27] are presented in Tables S1 and S2 and equation (S1), respectively (see the Supplementary material). The generation cost for the optimal 24 h DED (without solar

Table 4: Results of 2-tailed tests showing the solar load correlation coefficients and P values of various load profiles (LPs) under average, abundant, and scarce solar resource conditions.

LP	Average		Abundant		Scarce	
	Coefficient	P value	Coefficient	P value	Coefficient	P value
LP1	0.539**	0.007	0.558**	0.005	0.486*	0.016
LP2	0.458*	0.024	0.476*	0.019	0.433*	0.035
LP3	0.292	0.167	0.306	0.145	0.313	0.136
LP4	-0.006	0.979	0.003	0.991	0.083	0.701

*Correlation is significant at the 0.05 level (2-tailed). **Correlation is significant at the 0.01 level (2-tailed).

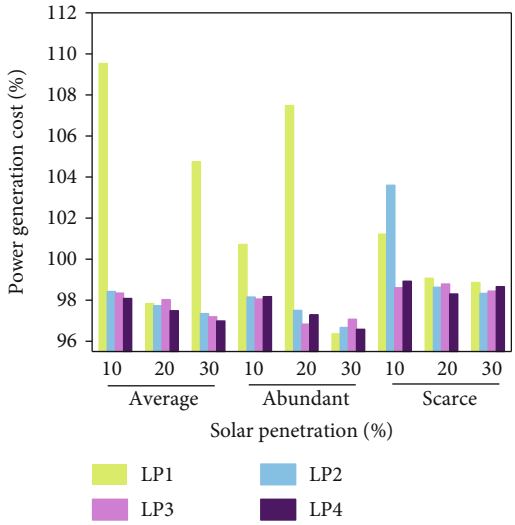

Figure 3: Power generation costs for the 24 h DEDs of the various load profiles (LPs) under average, abundant, and scarce solar resource conditions.

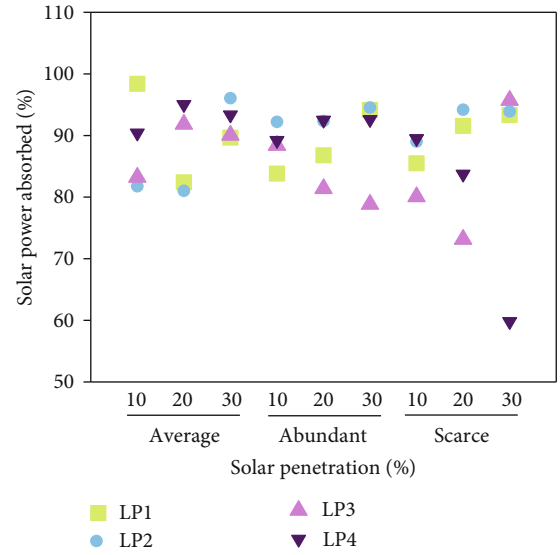

Figure 4: Solar power absorption levels for the 24 h DEDs of the load profiles (LPs) under average, abundant, and scarce solar resource conditions.

PV) was $13,616.40/day, which is comparable to the $13,555/day reported in [27]. The detailed results of the optimal 24 h DED of the thermal generation units using PSO are reported in Table S3 (see the Supplementary material). However, note that the focus of this study is not to introduce a new optimization algorithm but rather to implement an existing optimization algorithm to investigate the different levels of daytime peak loads under varying solar penetration conditions in solar-integrated power systems in order to improve the power generation cost and mitigate the challenges related to solar variation.

4. Results and Discussion

The results of the power generation costs of the 24 h DED for various load profiles (LPs) are presented as percentages based on a reference case (i.e., the initial load profile, LP1) in which there was no solar PV in the DED (Figure 3). As shown in Figure 3, the power generation costs decreased with increasing solar penetration for LP2, LP3, and LP4.

This reduction in the generation cost with increasing solar penetration can be attributed to the continuous displacement of the thermal generation units with marginally higher generation costs than the solar PV as a result of the solar power absorbed (Figure 4) [28]. Additionally, LP4, which had the lowest solar load correlation coefficient, exhibited the lowest generation costs under average solar resource conditions (Table 4).

Table 5: Load factors of various load profiles (LPs).

LP1	LP2	LP3	LP4
0.753	0.792	0.836	0.859

The minimum generation cost associated with LP4 was supported by the results of several other studies that have shown that load profile flattening can improve the generation costs of solar-integrated power systems [29, 30]. As a confirmation, the load factors, which are indicators of the flatness of the LPs, were estimated for the various LPs (Table 5) [31]. The high load factor of LP4, which was greater than those of the other load profiles, was also consistent with the results obtained above.

However, at the 10% and 20% solar penetration levels under abundant solar resource conditions, LP3, which had a higher positive solar load correlation coefficient than LP4,

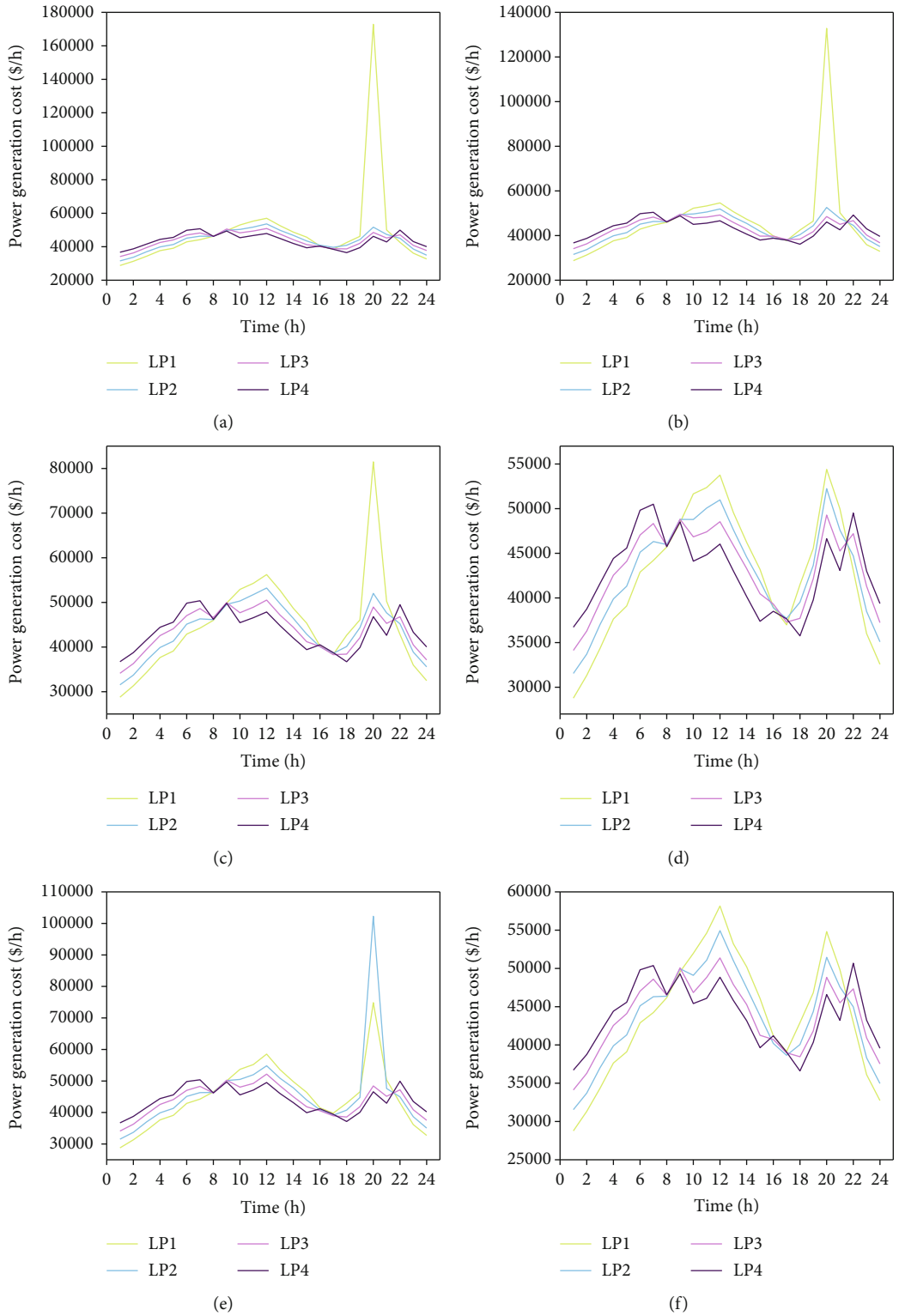

Figure 5: Hourly power generation costs for the 24 h DEDs of the load profiles (LPs) under (a) 10% average, (b) 30% average, (c) 10% abundant, (d) 30% abundant, (e) 10% scarce, and (f) 30% scarce solar penetration levels and resource conditions.

exhibited the best generation cost performance among the various load profiles. This inconsistency is likely related to the changes in the solar load correlation coefficient of LP4 from a negative to a positive value (Table 4). According to Chaiamarit and Nuchprayoon [18], variable RE sources such as solar PV have a time-varying impact on system performance and can lead to changes in the generation cost performance, such as those observed for LP3 and LP4, under average and abundant solar resource conditions.

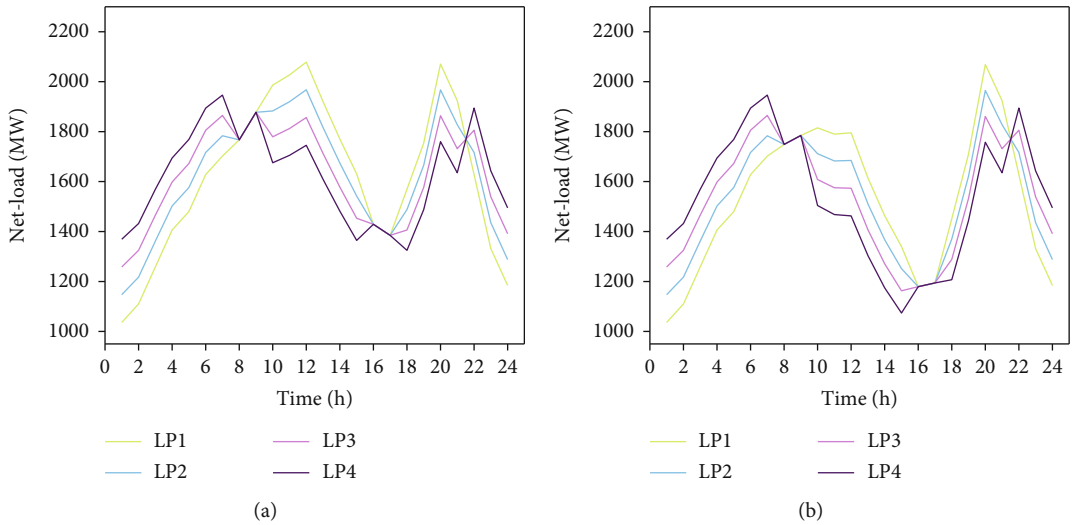

Figure 6: Net load curves of the load profiles (LPs) for (a) 10% and (b) 30% solar penetration levels and abundant solar resource conditions.

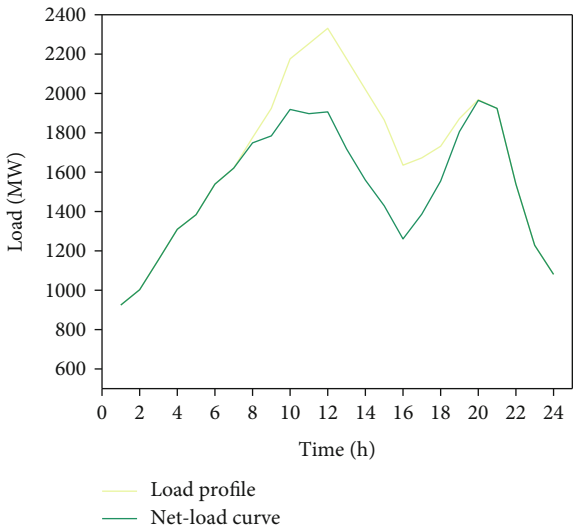

Figure 7: Twenty-four-hour load profile and net load curve of LP5 at 30% solar penetration under abundant solar resource conditions.

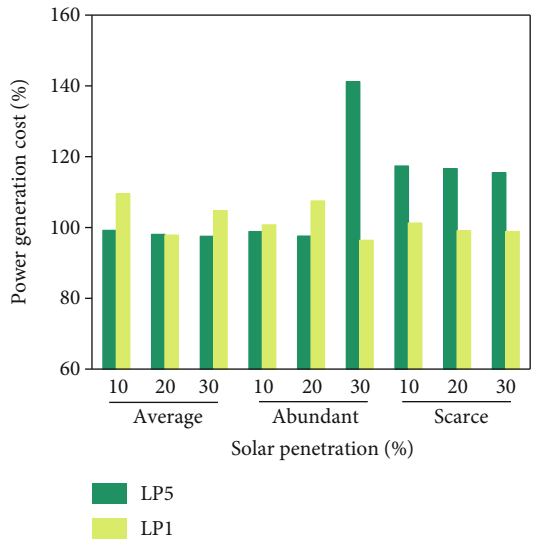

Figure 8: Power generation costs of the 24 h DED for LP5 and LP1 under average, abundant, and scarce solar resource conditions.

Table 6: Results of 2-tailed tests showing the solar load correlation coefficients and P values of LP5 under average, abundant, and scarce solar resource conditions.

Average		Abundant		Scarce	
Coefficient	P value	Coefficient	P value	Coefficient	P value
0.652**	0.001	0.673**	0.001	0.567**	0.004

**Correlation is significant at the 0.01 level (2-tailed).

Moreover, LP1 (with the highest positive solar load correlation coefficient) exhibited the worst generation costs, characterized by surges in most cases. Studies have shown that the absorption of solar power can shift peak loads to other periods of the day when solar power diminishes [2, 15]. This possible load shift might have exacerbated the already existing peak at 20 h, making it impossible for the dispatchable generation units to ramp up to meet the rising load demand from 19 h to 20 h and violating the supply-demand balance requirement. Consequently, the penalty factor adopted in this study resulted in the highest generation costs for LP1, which was characterized by surges (Figure 5).

This finding indicates that LPs with high daytime peak loads could lead to operational challenges during the evening load peaks in systems where dispatchable generation units do not have adequate ramping capability and can have adverse effects on generation costs. Moreover, LPs with evening load peaks are common and typically characterize residential consumption patterns [9, 16, 32]. Therefore, in the utilization of grid-integrated solar PV, taking precautionary measures during evening load peaks in power systems with high daytime peak loads could become necessary. In this regard, the lack of supply-demand balance requirement violations in the

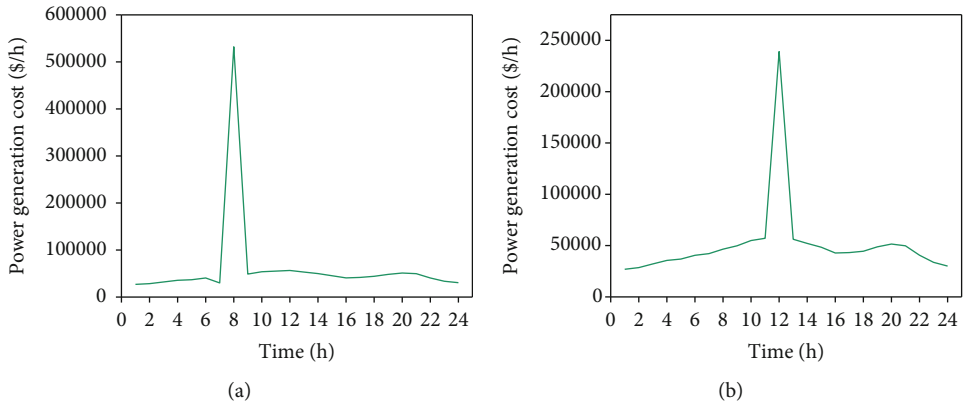

Figure 9: Hourly power generation costs of the 24 h DED for LP5 at 30% solar penetration under (a) abundant and (b) scarce solar resource conditions.

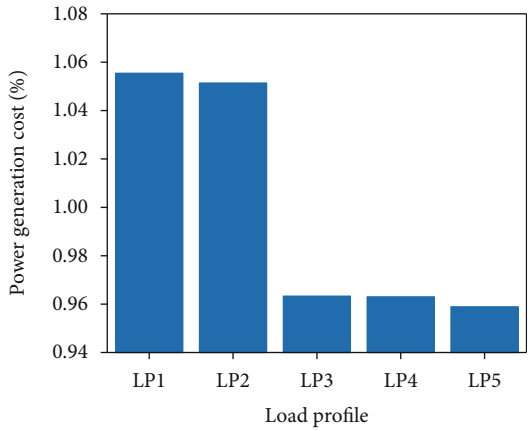

Figure 10: Power generation costs of the 24 h DEDs of the various load profiles (LPs) at 40% solar penetration under abundant solar resource conditions.

other LPs suggests that adopting demand-side management (DSM) techniques to reduce evening load peaks could solve the ramping problem.

However, at 30% solar penetration under abundant solar resource conditions, LP1 exhibited the most cost-effective load profile among the various load profiles, with a generation cost of 96.36%. This observation is likely related to the more extensive effects of high solar power penetration on the characteristics of LP1 and LP2 than on those of LP3 and LP4. Thus, Figures 6(a) and 6(b) illustrate the potential impact of solar PV on the LPs as the solar penetration increases from 10% to 30% using the net load concept [13, 18]. The figures show that there was a notable reduction in the daytime loads, particularly the daytime peak loads of LP1 and LP2 compared to those of LP3 and LP4, as the solar penetration increased from 10% to 30%, which agrees with the previous results.

Similarly, the obvious changes in the characteristics of LP2 are attributable to the considerable reduction in the generation cost from 97.5% to 96.67% as the solar penetration increased from 20% to 30% under abundant solar conditions. Conversely, the generation cost of LP3 increased by 0.24% as the solar penetration increased from 20% to 30%. The results obtained under the high solar penetration condition agreed with those in previous studies [8, 10, 11], which found that improving the daytime loads improved the generation costs of solar-integrated power systems.

Moreover, the different effects of solar PV on various LPs as the solar penetration increased from 10% to 30% under abundant solar conditions aligned with those of other studies, in which a significant share of variable renewable sources in power systems altered the original load characteristics [15–18].

Additionally, the results of violating the supply-demand balance requirements under relatively low solar penetration conditions (i.e., 10% penetration) in LP4 due to the inadequate ramping capability of the dispatchable generation units agreed with the findings in Ref. [16]. Notably, Ref. [16] found that even low penetration levels of solar PV could result in a high demand for the generation system ramping capability. It is worth noting that, at 10% solar penetration under scarce solar conditions, the supply-demand balance requirements were violated in LP2 due to ramping challenges in the generation units (Figure 5(e)). This observation could be related to undulations in the scarce solar resource condition profile compared to the bell-shaped average and abundant solar resource condition profiles (Figure 2).

Likewise, the undulating shape of the scarce solar resource condition profile may be the reason for the relatively irregular power generation cost performance observed for the various LPs under the scarce solar condition compared to those observed under the average and abundant solar conditions.

Note, however, that the load profile with the highest daytime peak loads (LP1) within the solar PV generation hours did not necessarily exhibit superior solar power absorption performance compared with the other load profiles in most scenarios (Figure 4). For instance, at 30% solar penetration under average solar conditions, the solar power absorption in LP1 was 89.7%, compared to 93.3% in LP4. This result is inconsistent with those in Refs. [7, 8], which found that improving the daytime loads improved the solar power absorption, and might have been caused by factors such as

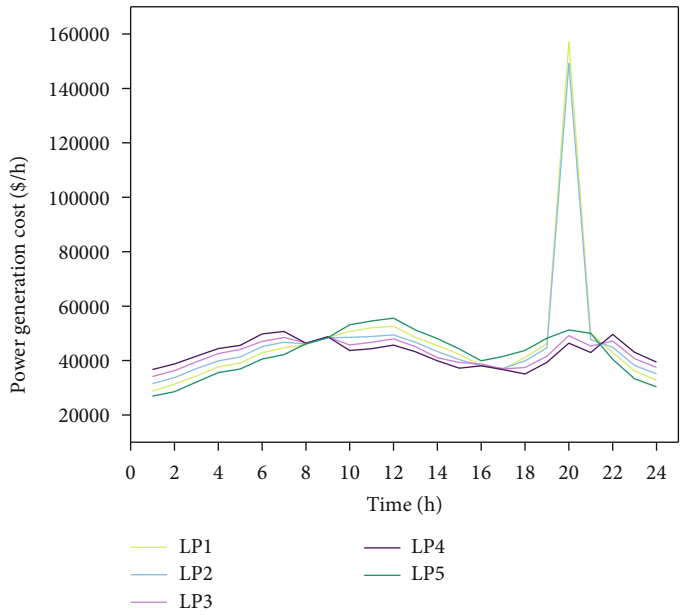

Figure 11: Hourly power generation costs of the 24 h DEDs of the load profiles (LPs) at 40% solar penetration under abundant solar resource conditions.

the net load characteristics, the ramping capability of the thermal generation units, and the availability of dispatchable generation units with marginally higher generation costs than solar PV [2, 28].

To further investigate the power generation costs of LPs as the positive solar load correlation coefficients increased, 5% of each load was shifted from the periods from 1 h to 7 h, 20 h, and from 22 h to 24 h to the period from 10 h to 19 h to obtain LP5. Figure 7 shows the 24 h load profile and net load curve of LP5 at 30% solar penetration under abundant solar resource conditions. In addition, Table 6 presents the solar load correlation coefficients and P values of LP5 under average, scarce, and abundant solar resource conditions. The results of the power generation costs of the 24 h DED of LP5 compared to those of LP1 are shown in Figure 8.

Figure 8 shows that LP5 exhibited lower generation costs than LP1 in most cases under average and abundant solar resource conditions. This observation could be related to the higher positive solar load correlation coefficient of LP5 than of LP1. However, at 30% solar penetration under abundant solar resource conditions, there was a violation of the supply-demand balance requirement in LP5, which consequently resulted in a surge in the generation cost due to the associated penalty (Figure 9(a)). However, unlike in previous cases in which the violation occurred during the evening hours (20 h), the violation in this case occurred at 8 h, even though the net load curve of LP5 suggested a higher evening peak (20 h) than the morning peak (10 h). Janko et al. [16] made a similar unusual observation in their study. Moreover, this result indicates that the operational challenges that could arise in LPs with high daytime peaks in solar-integrated power systems could also occur in parts of the day other than the evening peak period, as was previously observed.

The higher costs of generation in LP5 than in LP1 in all scenarios under scarce solar resource conditions were due to the violation of the supply-demand balance requirements and could be associated with the low quantity of solar power generated in hour 12 (Figure 9(b)). The sudden drop in solar irradiation from 11 h to 12 h in the scarce solar condition scenario might have resulted in further ramping required for the dispatchable generation units in LP5, which had higher daytime loads than LP1. Consequently, the insufficient ramping capability of the generation units resulted in the extensive violations observed in LP5.

Furthermore, solar penetration was increased to 40% to observe the generation cost performances for the various LPs. Figure 10 shows the power generation costs of the 24 h DEDs of the various LPs at 40% solar penetration under abundant solar resource conditions. Notably, LP5 and LP1 exhibited the best and worst generation cost performances, respectively. The inferior generation cost of LP1 is attributable to the violation of the supply-demand balance constraints from 19 h to 20 h due to the ramping challenges associated with the generation units, as observed in previous scenarios (Figure 11). Similar violations were observed in LP2. The superior generation cost performance exhibited by LP5 under high solar penetration levels further agreed with the results of other studies, which found that increasing the daytime load decreased the power generation cost. However, the violation of the supply-demand balance requirement, which occurred in LP1, further confirmed the previous inference that increasing the daytime load to mitigate solar variation challenges has the potential to pose operational challenges that could adversely affect the generation costs of power systems with inadequate ramping capabilities. Based on the results obtained in this study, generally, LP4 was nominated as the best load

profile in terms of generation cost improvement. However, under the highest solar penetration conditions, LP5 was nominated as the best load profile. Moreover, it was also observed that with respect to the individual load profiles, the best generation cost varied with the solar penetration levels. For example, the least generation cost in LP2 and LP5 was observed under the 30% and 40% penetration levels, respectively. These outcomes suggested that the optimal solar PV penetration level depended on the load profile under consideration.

5. Conclusions

This simulation study focused on the generation cost improvement of a solar-integrated power system by exploring the generation cost performance for different LPs with various daytime peak loads under varying solar penetration conditions to mitigate the challenges of solar variations. The daytime peak loads during the solar PV generation period were determined by measuring the solar load correlation coefficients, and the generation costs were modelled as a single-objective DED task with the PSO method. The results showed that the lowest generation costs were associated with LPs with low solar load correlation coefficients, while the LPs with the highest positive solar load correlation coefficients exhibited the highest generation costs, which were related to violations of the supply-demand balance requirements in most cases. However, at high solar penetration levels, the LPs with the highest positive solar load correlation coefficients also exhibited the lowest generation costs among the various LPs. These outcomes suggest that improving daytime peak load management can reduce the generation costs at high levels of solar penetration. However, this solar variation mitigation technique may pose operational challenges with adverse effects on power generation costs in generation systems with inadequate ramping capabilities. It is therefore recommended that DSM techniques be applied to reduce evening peak loads, which may help overcome some of the operational challenges that arise in the utilization of this solar variation mitigation technique. This study could be useful for load planning in solar-integrated power systems.

Data Availability

The data used to support the findings of this study are included within the article and supplementary information file.

Conflicts of Interest

The authors declare that there is no conflict of interest regarding the publication of this paper.

Acknowledgments

This work was supported by the National Natural Science Foundation of China (no. 51876083).

Supplementary Materials

Table S1: characteristics of the six thermal generation units. Table S2: twenty-four-hour load demand profile for the six-unit test system. Table S3: results of the optimal 24 h DED of the thermal generation units using PSO. *(Supplementary Materials)*

References

[1] S. Comello, S. Reichelstein, and A. Sahoo, "The road ahead for solar PV power," *Renewable and Sustainable Energy Reviews*, vol. 92, pp. 744–756, 2018.

[2] U. Helman, "Economic and reliability benefits of solar plants," in *Renewable Energy Integration*, E. Jones, Ed., pp. 351–372, Elsevier, Amsterdam, 2017.

[3] T. Jamal, T. Urmee, M. Calais, G. Shafiullah, and C. Carter, "Technical challenges of PV deployment into remote Australian electricity networks: a review," *Renewable and Sustainable Energy Reviews*, vol. 77, pp. 1309–1325, 2017.

[4] G. Shafiullah, M. T. Arif, and A. M. Oo, "Mitigation strategies to minimize potential technical challenges of renewable energy integration," *Sustainable Energy Technologies and Assessments*, vol. 25, pp. 24–42, 2018.

[5] M. A. Shoeb, F. Shahnia, and G. Shafiullah, "A multilayer and event-triggered voltage and frequency management technique for microgrid's central controller considering operational and sustainability aspects," *IEEE Transactions on Smart Grid*, vol. 10, no. 5, pp. 5136–5151, 2018.

[6] K. Karunanithi, S. Saravanan, B. Prabakar, S. Kannan, and C. Thangaraj, "Integration of demand and supply side management strategies in generation expansion planning," *Renewable and Sustainable Energy Reviews*, vol. 73, pp. 966–982, 2017.

[7] N. Stodola and V. Modi, "Penetration of solar power without storage," *Energy Policy*, vol. 37, no. 11, pp. 4730–4736, 2009.

[8] A. M. Hasan and S. A. Chowdhury, "Solar diesel hybrid minigrid design considerations: Bangladesh perspective," in *3rd International Conference on the Developments in Renewable Energy Technology (ICDRET)*, pp. 1–4, Dhaka, Bangladesh, July 2014.

[9] S. Fezai and J. Belhadj, "Load profile impact on a stand-alone photovoltaic system," in *2016 7th International Renewable Energy Congress (IREC)*, pp. 1–6, Hammamet, Tunisia, May 2016.

[10] A. Rose, R. Stoner, and I. Pérez-Arriaga, "Prospects for grid-connected solar PV in Kenya: a systems approach," *Applied Energy*, vol. 161, pp. 583–590, 2016.

[11] B. O. Bilal, V. Sambou, P. Ndiaye, C. Kébé, and M. Ndongo, "Study of the influence of load profile variation on the optimal sizing of a standalone hybrid PV/wind/battery/diesel system," *Energy Procedia*, vol. 36, pp. 1265–1275, 2013.

[12] Y. Liu, D. Yu, and Y. Liu, "Potential of grid-connected solar PV without storage," in *2010 International Conference on Power System Technology (POWERCON)*, pp. 1–5, Hangzhou, China, October 2010.

[13] I. S. Bayram, F. Saffouri, and M. Koc, "Generation, analysis, and applications of high resolution electricity load profiles in Qatar," *Journal of Cleaner Production*, vol. 183, pp. 527–543, 2018.

[14] M. George and R. Banerjee, "A methodology for analysis of impacts of grid integration of renewable energy," *Energy Policy*, vol. 39, no. 3, pp. 1265–1276, 2011.

[15] E. Johnson, R. Beppler, C. Blackburn, B. Staver, M. Brown, and D. Matisoff, "Peak shifting and cross-class subsidization: the impacts of solar PV on changes in electricity costs," *Energy Policy*, vol. 106, pp. 436–444, 2017.

[16] S. A. Janko, M. R. Arnold, and N. G. Johnson, "Implications of high-penetration renewables for ratepayers and utilities in the residential solar photovoltaic (PV) market," *Applied Energy*, vol. 180, pp. 37–51, 2016.

[17] B. Asare-Bediako, W. Kling, and P. Ribeiro, "Future residential load profiles: scenario-based analysis of high penetration of heavy loads and distributed generation," *Energy and Buildings*, vol. 75, pp. 228–238, 2014.

[18] K. Chaiamarit and S. Nuchprayoon, "Impact assessment of renewable generation on electricity demand characteristics," *Renewable and Sustainable Energy Reviews*, vol. 39, pp. 995–1004, 2014.

[19] K. Vaisakh, P. Praveena, S. R. M. Rao, and K. Meah, "Solving dynamic economic dispatch problem with security constraints using bacterial foraging PSO-DE algorithm," *International Journal of Electrical Power and Energy Systems*, vol. 39, no. 1, pp. 56–67, 2012.

[20] Z. Hasan and M. E. El-Hawary, "Economic dispatch at peak load using load reduction for smart grid network," in *2016 IEEE Electrical Power and Energy Conference (EPEC)*, pp. 1–5, Ottawa, ON, October 2016.

[21] S. Ramabhotla, S. Bayne, and M. Giesselmann, "Operation and maintenance cost optimization in the grid connected mode of microgrid," in *2016 IEEE Green Technologies Conference (GreenTech)*, pp. 56–61, Kansas City, MO, USA, April 2016.

[22] L. Jebaraj, C. Venkatesan, I. Soubache, and C. C. A. Rajan, "Application of differential evolution algorithm in static and dynamic economic or emission dispatch problem: a review," *Renewable and Sustainable Energy Reviews*, vol. 77, pp. 1206–1220, 2017.

[23] M. Nazari-Heris, S. Abapour, and B. Mohammadi-Ivatloo, "Optimal economic dispatch of FC-CHP based heat and power micro-grids," *Applied Thermal Energy*, vol. 114, pp. 756–769, 2017.

[24] F. K. Dadzie, *Design of a grid connected photovoltaic system for KNUST and economic and environmental analysis of the designed system*, Master Thesis, Kwame Nkrumah University of Science and Technology, Kumasi, Ghana, 2008.

[25] G. Abbas, J. Gu, U. Farooq, M. U. Asad, and M. El-Hawary, "Solution of an economic dispatch problem through particle swarm optimization: a detailed survey-part I," *IEEE Access*, vol. 5, pp. 15105–15141, 2017.

[26] A. Abdelaziz, E. Ali, and S. A. Elazim, "Flower pollination algorithm to solve combined economic and emission dispatch problems," *Engineering Science and Technology, an International Journal*, vol. 19, no. 2, pp. 980–990, 2016.

[27] B. Lokeshgupta and S. Sivasubramani, "Multi-objective dynamic economic and emission dispatch with demand side management," *International Journal of Electrical Power & Energy Systems*, vol. 97, pp. 334–343, 2018.

[28] A. S. Brouwer, M. Van Den Broek, A. Seebregts, and A. Faaij, "Impacts of large-scale intermittent renewable energy sources on electricity systems, and how these can be modeled," *Renewable and Sustainable Energy Reviews*, vol. 33, pp. 443–466, 2014.

[29] K. Mahmud, M. J. Hossain, and G. E. Town, "Peak-load reduction by coordinated response of photovoltaics, battery storage, and electric vehicles," *IEEE Access*, vol. 6, pp. 29353–29365, 2018.

[30] N. Javaid, I. Ullah, M. Akbar et al., "An intelligent load management system with renewable energy integration for smart homes," *IEEE Access*, vol. 5, pp. 13587–13600, 2017.

[31] J. Surai and V. Surapatana, "Load factor improvement in industrial sector using load duration curves," in *2014 International Electrical Engineering Congress (iEECON)*, pp. 1–4, IEEE, Chonburi, Thailand, March 2014.

[32] D. D. Sharma and S. Singh, "Electrical load profile analysis and peak load assessment using clustering technique," in *2014 IEEE PES General Meeting Conference and Exposition*, pp. 1–5, National Harbor, MD, USA, July 2014.